Influence of gain dynamics on dissipative soliton interaction in the presence of a continuous wave

A. Niang, F. Amrani, M. Salhi, H. Leblond, and F. Sanchez
LUNAM Université, Université d'Angers, Laboratoire de Photonique d'Angers, EA 4464, 2 Boulevard Lavoisier, 49045 Angers Cedex 01, France
(Received 31 March 2015; published 17 September 2015)

We investigate the effect of the gain dynamics on the motion and interactions of solitons in the frame of a complex Ginzburg-Landau-type model, which accounts for dissipative soliton formation and propagation in a ring fiber laser. It is shown that the gain dynamics modifies the soliton velocity and their interactions. In the presence of an injected continuous wave, an initial crystal of a few solitons gets broken, either into bunches or into individual solitons. Quasielastic collisions analogous to Newton's cradle have been seen. The soliton set may evolve into gas, solitons, or harmonic mode-locked patterns. The time jitter present in the last situation has been considered.

DOI: 10.1103/PhysRevA.92.033831 PACS number(s): 42.65.Tg, 05.45.Yv, 42.55.Wd

I. INTRODUCTION

Dissipative solitons are robust entities which arise in many physical situations. As conservative solitons, which have been considered as interesting candidates for elementary particles, they may have particlelike behavior. Laser cavities are the ideal experimental frame for the study of dissipative soliton interactions since they make it possible to build many various situations, which show a huge quantity of different behaviors. In fiber lasers, using various mode-locking processes, large numbers of solitons can be produced, forming a multipulse pattern [1].

It has been shown that several features of high-power wave propagation, such as supercontinuum generation [2] or optical rogue waves [3], could be explained from interactions of a large numbers of solitons. Further, such patterns have practical applications to produce ultrahigh-repetition rate pulsed laser sources [4]. The knowledge of the interactions between solitons is then essential to stabilize the pulse train.

On the other hand, experiments have shown that they exhibit collective behaviors comparable to states of matter [5–7]. Gas, liquids, and crystals of solitons have been evidenced, but also more exotic behaviors such as the soliton rain [8] or harmonic mode locking of soliton crystals [9]. Thus, the modeling of the multisoliton interaction is an important issue, from both the fundamental and the applicative points of view.

Harmonic mode locking is usually considered as the result of a purely repulsive interaction between moving pulses, which thus arrange themselves in order to maximize the distance between neighboring pulses. It has been observed that a continuous component was generally present together with the regularly distributed short pulses [1,9–11]. The possibility of controlling such a component by externally injecting it has been recently investigated experimentally [4]. From the theoretical point of view, the soliton motion which is involved in this process, and also necessary for soliton gas formation, is, in principle, prohibited in the complex Ginzburg-Landau (CGL) equation due to the spectral filtering (the finite gain bandwidth), while it is present in the experiments (notice, however, that some computation made it possible to retrieve a soliton gas behavior within the frame of CGL [12]). It has been shown that an external source of continuous wave can induce soliton motion and lead to the formation of the various states of matter of solitons, depending on its frequency and amplitude [13].

However, although the CGL model driven by a continuous wave makes it possible to reproduce the experimental observations in what regards the soliton crystal, gas, and liquid, to our knowledge, it fails to describe the harmonic mode-locking regime. It seems that purely repulsive interactions are not present within this model. On the other hand, two very important effects due to the dynamics of gain are not taken into account by the CGL equation. One is that the total energy in the cavity is limited and can be controlled by the pumping rate. Consequently, there is some limitation in the number of pulses, which is not taken into accounted by the CGL equation. The second is that the gain is nonconstant all along the pulse train, since each soliton takes some energy, and there is less left for the following one. This induces a dissymmetry and effective long-range interaction [14]. Hence, we may think that gain dynamics can be responsible for harmonic mode locking and will support this statement by numerical study of a CGL-type model.

The aim of the present paper is to investigate how these two effects impact soliton motion or, more exactly, how the gain dynamics (the second effect) affects soliton motion within a pulse train whose length is fixed owing to the gain saturation (the first effect). After having presented the model (Sec. II), we first discuss in Sec. III the effect of the integral term which accounts for gain dynamics on the motion of the solitons of CGL equation. In Sec. IV, we retrieve with this more complete model, the generation of soliton gas, liquid, or crystal already obtained with a simpler model in [13]. In Sec. V we see that the model makes it possible to obtain the harmonic mode locking, as observed in experiments [4]. A remarkable feature of the model is that it presents jitter; two different jitter types are identified in Sec. VI, after which we conclude.

II. MODEL AND GAIN DYNAMICS

The evolution of dissipative soliton in the cavity of a mode-locked fiber laser, where an external continuous wave is injected, can be modeled by the following CGL-type

equation:

$$\frac{\partial E}{\partial z} = \left(\frac{g_0}{1+\langle|E|^2\rangle/I_s} - r\right)E + \left(\beta + i\frac{D}{2}\right)\frac{\partial^2 E}{\partial t^2} + (\varepsilon + i)E|E|^2 + (\mu + i\nu)E|E|^4 - \Gamma E\int_{-\infty}^{t}(|E|^2 - \langle|E|^2\rangle)dt' + A\exp(-i\Delta\omega_0 t). \quad (1)$$

The parameters β, D, ε, μ, and ν have their standard meaning in the context of the dimensionless CGL equation: They represent, respectively, the spectral gain filtering, the dispersion, the saturation of the linear absorption, the quintic nonlinear gain, and the quintic nonlinear index in a normalized way. A simplified form of this model, the cubic CGL equation [i.e., Eq. (1) with $1/I_s = \Gamma = A = \mu = \nu = 0$], was derived from the equations which describe propagation in a fiber in [15] in the case of a fiber laser mode locked by nonlinear rotation of the polarization and in [16] for the figure-eight laser. It is nothing but the evolution equation related to Haus master mode-locking equation [17]. The quintic CGL equation [i.e., Eq. (1), with $1/I_s = \Gamma = A = 0$, but nonvanishing μ, ν] was derived in [18,19]. All cited papers provide explicit expressions of the coefficients of the CGL equation in terms of laser characteristics.

The gain saturation term involves the gain coefficient g_0, while r yields for linear losses and I_s for saturation intensity. The averaged intensity is $\langle|E|^2\rangle = \frac{1}{T}\int|E|^2dt$, where T is the length of the cavity (the round-trip time) or the length of the numerical box. Notice that, multiplied by the effective area of mode, the average intensity $\langle|E|^2\rangle$ is nothing but the average power in the usual sense. The relaxation time of the gain is rather long (about 10 ms for Er/Yb doped fibers), and consequently the power should, in principle, be averaged over a large number of round trips. However, we restrict to the average over one cavity length for technical reasons. This approximation is used very often and gives results in accordance with experiments.

The integral term accounts for the gain dynamics, the fast response of the gain. Γ is proportional to the gain (in principle, it should be the saturated gain $[g_0/(1+\int|E|^2dt/W_s) - r]$, but the saturation of this term can be considered as a higher-order correction and is omitted for sake of simplicity). A derivation of this contribution term by means of a perturbative approach has been provided in Ref. [20]. The last term is a source one, accounting for the injected continuous wave, as in Ref. [13].

We solve the initial value problem for Eq. (1) by means of a standard fourth-order Runge-Kutta algorithm in the frequency domain. The nonlinear terms are computed by inverse and direct fast Fourier transforms at each substep of the scheme, the integral in the saturation term is evaluated by a mere summation, the antiderivative in the fast gain response term is computed in the spectral domain. The adequate definition of the antiderivative is that the mean value of the integrand must be removed first and that the mean value of the antiderivative must be zero: It is exactly what provides the computation in the spectral domain.

Evaluation of the values of parameters corresponding to a given experiment is a difficult task, which had been performed in Ref. [20] (however, quintic nonlinear terms and injected waves were not considered there). From the experimental point of view, β measures the bandwidth of the gain and losses. It thus essentially depends on the nature of the amplifying medium, but the bandwidth can be modified using spectral filters, the change leading normally to a narrowing of the bandwidth, i.e., an increase of β. The nonlinear gain parameters ϵ and μ characterize the saturable absorber used. When using the nonlinear rotation of the polarization, they are modified by adjustment of polarization controllers. ν normally arises from the fifth-order nonlinear susceptibility $\chi^{(5)}$ of the medium, but an effective effect can be expected in some situations. It was shown to be zero in the situation and within the approximations of Ref. [18]. Due to the normalization, all parameters depend also on the dispersion parameter, on the nonlinear index n_2, and on one free adjustment parameter. Owing to this great complexity, in order to remain very general, we use arbitrary (*ad hoc*) values of the normalized parameters, as $D = 1$ (anomalous dispersion regime as in experiment), $\nu = 0$, $\beta = 0.5$, $\varepsilon = 0.4$, and $\mu = -0.05$. This choice ensures that the fundamental soliton is stable, which occurs in the experimental situation we intend to model.

We use periodic boundary conditions. In some sense, it reproduces the experimental situation, since the real cavity makes a loop. However, the real cavity length is much larger than the numerical one, with respect to the soliton duration. Some features of the numerical model can be interpreted in terms of finite cavity length, but the fact that the order of magnitude of the cavity length is not the one which is relevant with respect to experiment must be kept in mind. Hence, a model independent of the numerical box size should be welcome.

However, this independence can be understood in two different ways, namely, either the number of pulses, or their density (number of pulses by unit length of cavity) can be conserved as T is changed. We have written the equation according to the second option. Questions come from gain saturation and gain dynamics (only). Regarding saturation, the model is written in a way that is independent of the box size, since we consider the average intensity instead of the energy. However, variations still occur when the box size is modified. They seem to originate in the fact that the number of pulses depends on I_s in a very subtle way, and the computation of the integral $\int|E|^2dt$ is not very accurate, depending on spatial resolution. Concretely, a few percent correction of the value of I_s may be necessary to get the same result when doubling or halving the box size.

The integral term is, in principle, independent of the box size, too, but, in practice, some difficulties arise: For small values of T, the mismatch between the eigenperiod of the pulse train (distance between pulses) and the box size induces low-frequency components, corresponding to a slow increase of the gain (this integral gain term), followed by a rapid decrease. A change of the box size may invert the direction of this variation.

III. PULSE MOTION DUE TO GAIN DYNAMICS

Before we investigate how the gain dynamics can modify the collective behavior of solitons, it is worth considering, from the very mathematical point view, how the term which represents gain dynamics in the model, i.e., the integral term

in Eq. (1), affects the motion of a single soliton by itself. Hence, we consider Eq. (1) without source term ($A = 0$) and without gain saturation ($I_s = \infty$). The algebraic excess of gain is fixed as $\delta = (g_0 - r) = -0.01$. The numerical cavity length is $T = 200$. The initial data is built by linear superposition of two solitons of the pure CGL equation [i.e., Eq. (1) with the above parameters and $\Gamma = 0$], computed numerically. The coefficient Γ depends essentially on the gain and on its saturation parameter [20], but also on the normalization. Although it may considerably vary depending on the experimental conditions, including the pumping rate, there is no straightforward way to adjust it in an experiment. It is, however, always a small parameter.

The fast response of gain induces a slow motion of the pulse. The inverse velocity $w = dt/dz$ is about -0.0058 for $\Gamma = 0.006$ and -0.0028 for $\Gamma = 0.007$. Globally, it tends to increase with Γ, but not in a monotonic way. Notice that, since Eq. (1) is written in a frame moving at the linear group velocity v_g of the waves, $w = \Delta(1/v_g)$ is a correction to the inverse of the pulse velocity. It is negative, and, consequently, the correction to the pulse velocity is positive and the gain dynamics increases the speed. Indeed, it corresponds to some consumption of the pump energy by the pulse; hence, the gain is higher in front of the pulse than behind it. The amplitude of the pulse front increases due to enhanced gain, and the amplitude of the back is reduced correspondingly. This yields an effective pulse motion towards its front, i.e., an increase of the speed.

An instability is observed, in the form of a set of new pulses which arise in front of the initial pulses (on the side of the negative t) and quickly disappear. The process of unstable pulse emission tends to repeat along the whole cavity; after little more than one round trip the pulses tend to stabilize and a multipulse pattern forms (Fig. 1). For larger Γ, the instability increases: Secondary pulses form sooner and they vanish faster. From about $\Gamma = 0.03$ on, the final stabilization of the pulse train does not occur any more, and pulses are created and vanish permanently (see Fig. 2). The generated pulses vanish so quickly that they have no time to propagate

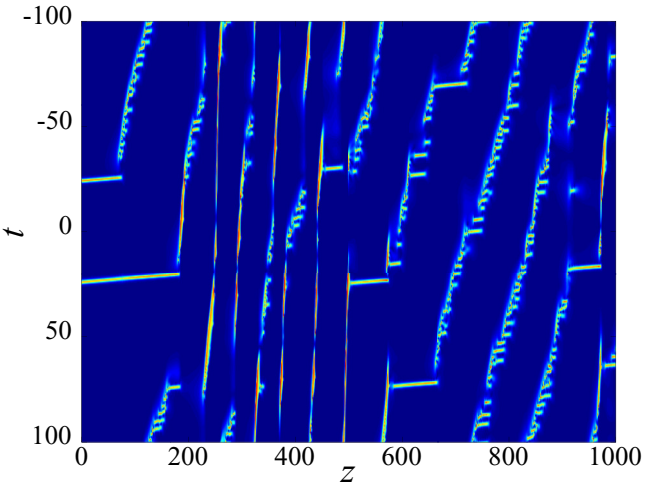

FIG. 2. (Color online) Instability with $\Gamma = 0.03$: permanent generation and vanishing of pulses.

any more, and the process of generation and vanishing of the pulses turns into an effective motion of the pulse. The inverse velocity w of this motion is very large with respect to the initial induced velocity discussed above (see Fig. 3). For high values of Γ, the moving soliton turns to be unstable and vanishes, the whole solutions going toward the off state (not shown). It is thus seen that gain dynamics can induce soliton motion and even that, if it becomes larger, a fast apparent motion due to absorption and reemission is possible.

IV. INJECTED CONTINUOUS WAVE

We showed in [13] that the injected continuous wave is able to induce soliton motion and consequently make it possible to reproduce the collective behaviors as soliton liquid or gas in the frame of the CGL model. A question arises as to whether these results persist with the present, more complete, model and how they can be modified. Therefore, we now consider the joint effect of pulse propagation of both a continuous wave,

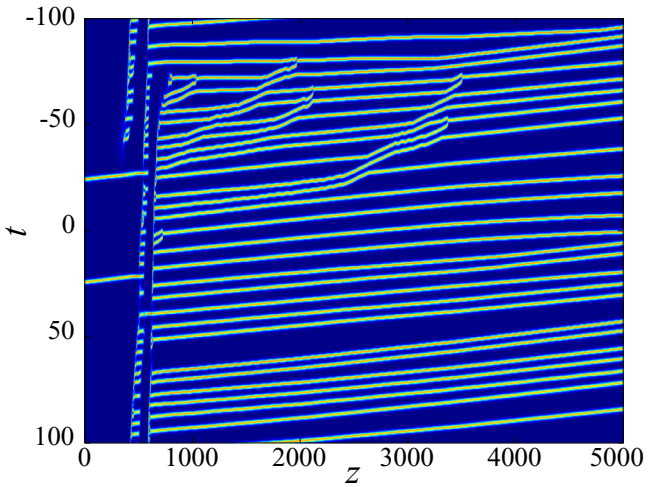

FIG. 1. (Color online) Instability with $\Gamma = 0.01$: generation of a long pulse train.

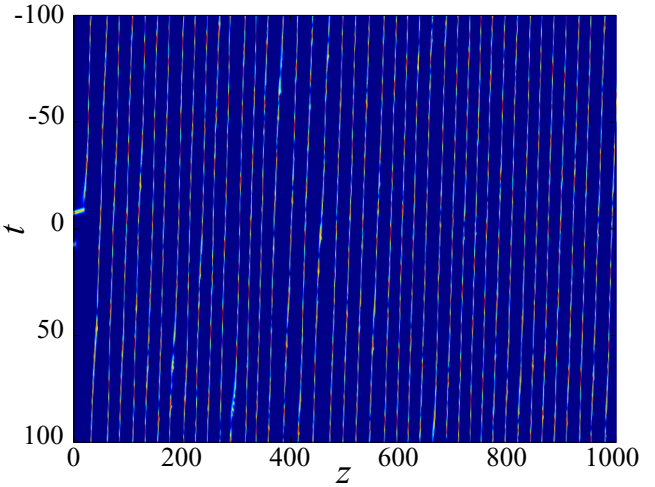

FIG. 3. (Color online) Motion due to pulse generation and vanishing, $\Gamma = 0.1$. The second initial pulse quickly vanishes.

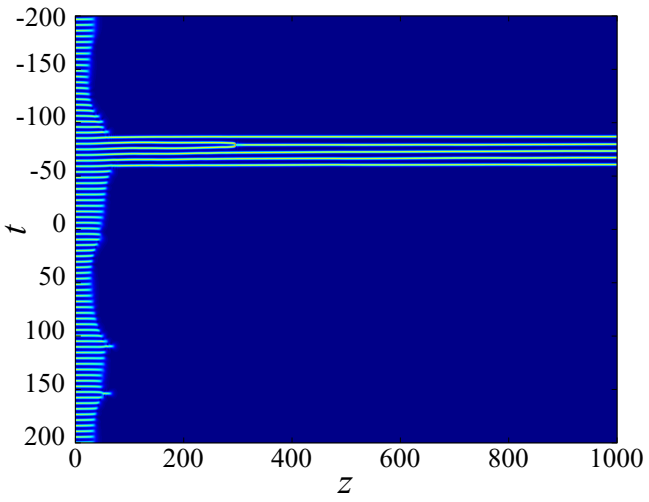

FIG. 4. (Color online) A bound state of five solitons which will be used as input for subsequent calculations; parameters: $A = 0$, $g_0 = 0.09$, $\Gamma = 0.0003$, $r = 0.2$, and $I_s = 0.025$.

which we control by injecting it, and the gain dynamics. It has been seen above for the gain dynamics and in [13] for the injected wave that both induce instabilities which results in a increase of the number of pulses, which will then be bounded by the numerical cavity length only. We intend here to inspect the propagation of a fixed number of pulses, smaller than the maximal one which can appear in the cavity: This requires a limitation of the pulse number, which is yielded by the gain saturation term. Most features presented in this section, which were not seen in [13], are due to this important difference between the present model and the nonsaturated model used in that reference.

Since the process is slow, very long propagation distances are needed, and therefore we restrict to moderate cavity length and temporal resolution. Without injected signal ($A = 0$), an adequate choice of the parameters (g_0, Γ, r, and I_s) makes it possible to obtain a bound state of four or five solitons, filling a small part of the computation box. An example is given in Fig. 4, obtained with $\Gamma = 0.0003$, $g_0 = 0.09$, $r = 0.2$, $I_s = 0.025$, and $T = 400$, the remaining parameters being the same as above. The parameters g_0 and Γ are, in principle, fixed by the laser characteristics. However, although values of parameters explicitly related to an experimental setup would be, in principle, preferable, owing to the great complexity of the relationship between experimental control parameters and the normalized parameters of the model (see Ref. [20]), we use in this paper *ad hoc* arbitrary values. Although, for technical reasons, we can consider here a small number of solitons only, we keep in mind that this bound state represents the crystal state observed in experiments with a much larger number of solitons.

We used this bound state (Fig. 4) as initial data to solve numerically Eq. (1). We chose a relatively small frequency shift $\Delta\nu_0 = \Delta\omega_0/2\pi = 0.1$, and we vary the amplitude A of the injected continuous wave, which is easily realized experimentally by adjusting the pumping rate of the injecting laser. It is not equivalent to consider the same five-soliton train in a shorter or in a longer numerical cavity. We considered here two different cavity lengths, $T = 400$ and 100, with the same saturation fluency $TI_s = 10$. The five-soliton bound state is stationary in both cases (but not completely stable for $T = 100$), but the intensity saturation is changed from $I_s = 0.025$ to 0.1, and consequently the equation is modified.

For $T = 400$ and $I_s = 0.025$, when the amplitude of the injected component is quite small (up to $A = 0.04$), nothing happens; the bound state does not change. In this case, the injected component has no visible effect on the behavior of the solitons. When the amplitude A ranges from 0.05 to 0.13, the bound state still exists, but the solitons acquire some speed. At moderately large amplitudes $A \geq 0.14$, the bound state breaks up, yielding two bunches of two and three solitons. These bunches occupy only part of the computation box, and the distance between them varies with the amplitude of the injected component. For strong injected amplitudes A, other solitons appear after some propagation distance, and may eventually fill the entire computation box. These pulses have different amplitudes, and their relative positions are not fixed. In this situation, the injected component supplies energy to the system. The model then does not describe a laser cavity controlled by a small injected signal, but rather resembles a passive cavity in which gain would have been added. The physical situation is thus completely different, even if the model is the same, and we do not consider it further hereafter. It is thus seen that the injected wave is able to strongly modify the interaction between solitons.

Changing $T = 400$ into 100 and $I_s = 0.025$ to 0.1 conserves the initial bound state of five solitons, which now occupies 3/10 of the numerical box, but it appreciably modifies the gain dynamics. $\Delta\nu_0 = \Delta\omega_0/2\pi$ is the detuning between the optical frequencies of the injecting laser and of the main cavity. In an experiment, it can be easily adjusted if a tunable laser is used as the injecting one. We fix then $\Delta\nu_0 = 0.1$ and vary the amplitude A of the injected wave. Several collective behaviors of the soliton set can be obtained. Typically, with respect to the above situation, the thresholds of the continuous wave amplitude A are lowered.

For low amplitudes ($A \leq 0.105$), the soliton bound state breaks up into two or three bunches. Collisions between the soliton bunches arise when they meet again due to periodicity. Some of these collisions are of quasielastic type: When one soliton hits the bunch, another leaves on the other side, as in a very short version of Newton's cradle. Such effect has already been observed for spatial dissipative solitons [21], and also in chains of conservative solitons created by fission of higher-order solitons [22]. In the latter case, the chain was much longer, and the symmetry was broken by the third-order dispersion. In the present paper, this role is played by the integral term accounting for gain dynamics. Figure 5 shows two typical examples. For readability, the numerical results are presented in a frame moving at some inverse speed w (given in the caption of each figure) close to the group velocity of the train, which is not the frame in which Eq. (1) is solved.

The soliton bunches can be phase locked or not. In the example of Fig. 5(a), phases vary linearly with z: There is no phase interaction, while in the example of Fig. 5(b), the solitons pairs can be phase locked between two collisions.

With moderately high amplitudes (between $A = 0.110$ and $A = 0.120$), two situations are observed. The pulses may fill

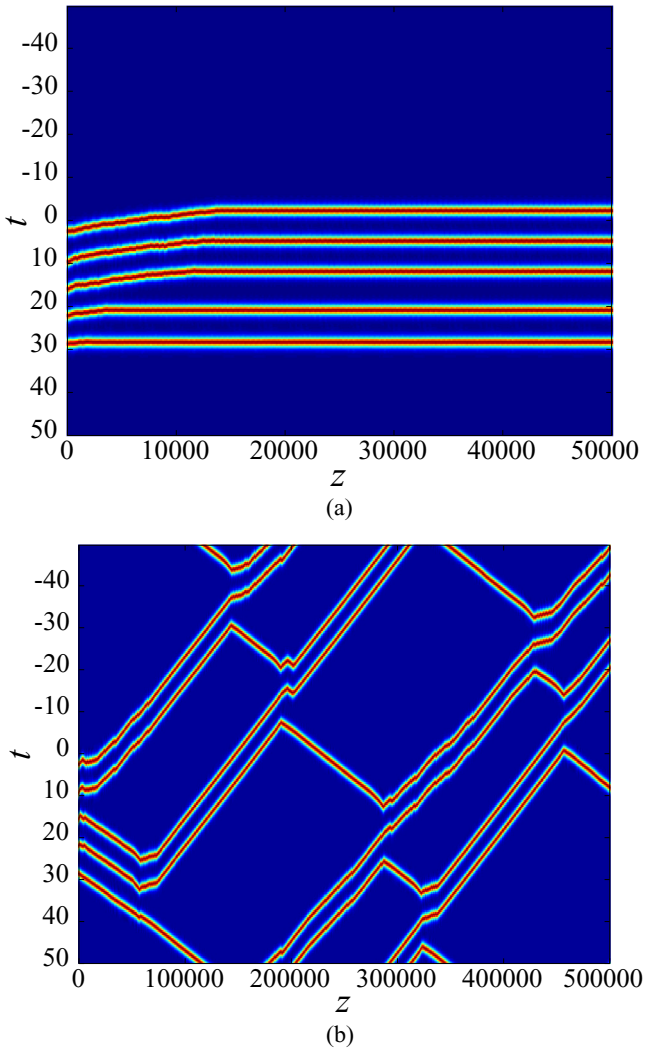

FIG. 5. (Color online) (a) Breaking of the initial bound state into two bunches, for $\Delta\nu_0 = 0.1$, $A = 0.005$, $w = 0$. (b) For a higher amplitude of the injected component $A = 0.020$, the three-pulse bunch breaks again into a pair and a soliton, which will collide elastically; $w = 0.0005$.

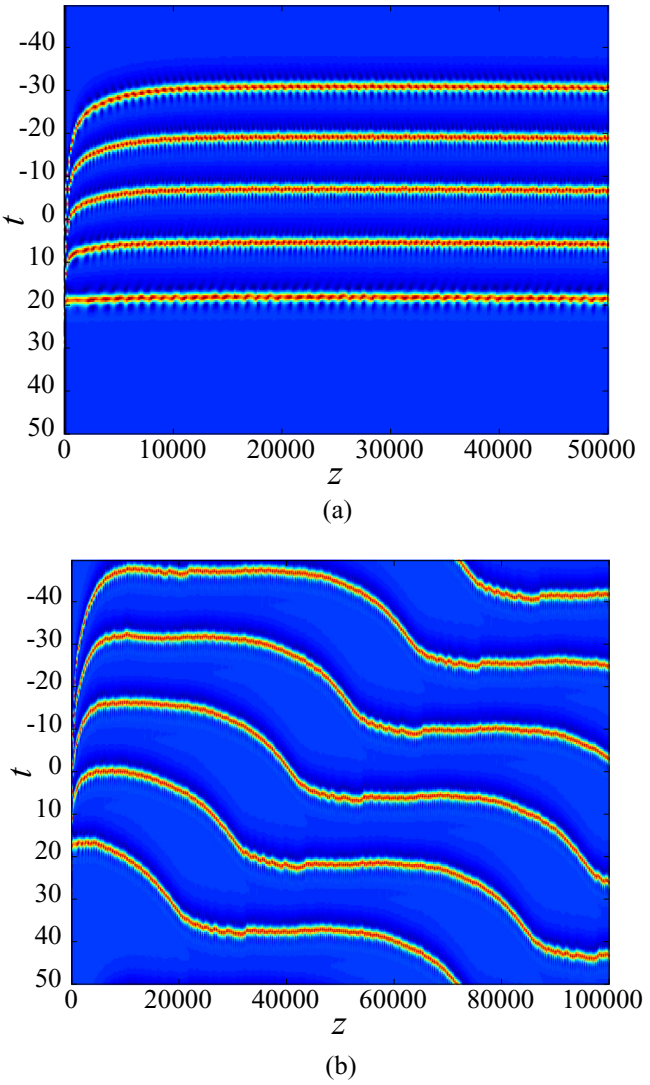

FIG. 6. (Color online) Evolution of an initial bound state (representing the crystal) to either (a) a liquid or (b) a gas of solitons depending on the value of the injected amplitude. Parameters are $\Delta\nu_0 = 0.1$ and (a) $A = 0.115$, $w = 0.058\,77$; (b) $A = 0.120$, $w = 0.070\,40$.

half of the box, being identical and almost exactly equidistant (locked in position), but in this case there is no phase locking between consecutive solitons. This is a condensed phase, but not regularly organized: We can refer to it as a liquid [Fig. 6(a)]. The other outcome is that the pulses fill the whole box, being in permanent motion; in this case, their amplitudes are irregular and the separation between two consecutive solitons is not fixed, as in a gas [Fig. 6(b)]. There is obviously no phase-locking either. We consider here a situation in which the number of solitons is fixed and do not fill the entire computation box, at least in condensed states. The situation, where the initial soliton crystal fills the entire computation box, was considered in [13]. In this case it was possible to consider a much larger number of solitons, since the propagation distance required to make apparent the crystal-liquid-gas transition is much less than the time characteristic to the long-range interaction between pulses we consider here. Using the same values of the parameters β, D, ε, μ, and ν as in the present paper and a fixed excess of linear gain $\delta = -0.01$, but much larger box size, we obtained, for $\Delta\nu_0 = 0.1$, a crystal of solitons for $A = 0.1$ and below, a liquid for $0.15 \leq A \leq 0.25$, and a gas for $A \geq 0.3$. The results were very close to the present ones; however, the values of the thresholds are not fully independent of box size, as mentioned above. Summarizing, we retrieve here the crystal-liquid-gas transition as in [13], but the saturation of the gain makes it possible to bring forward the condensate character of the liquid and crystal with respect to the dilute gas. In addition, other behaviors as crystal breaking have been observed.

V. HARMONIC MODE LOCKING

It may also happen that the bound state breaks into individual solitons, which can, in turn, fill the whole computation box, instead of bunches. When $A = 0.125$, the pulses occupy

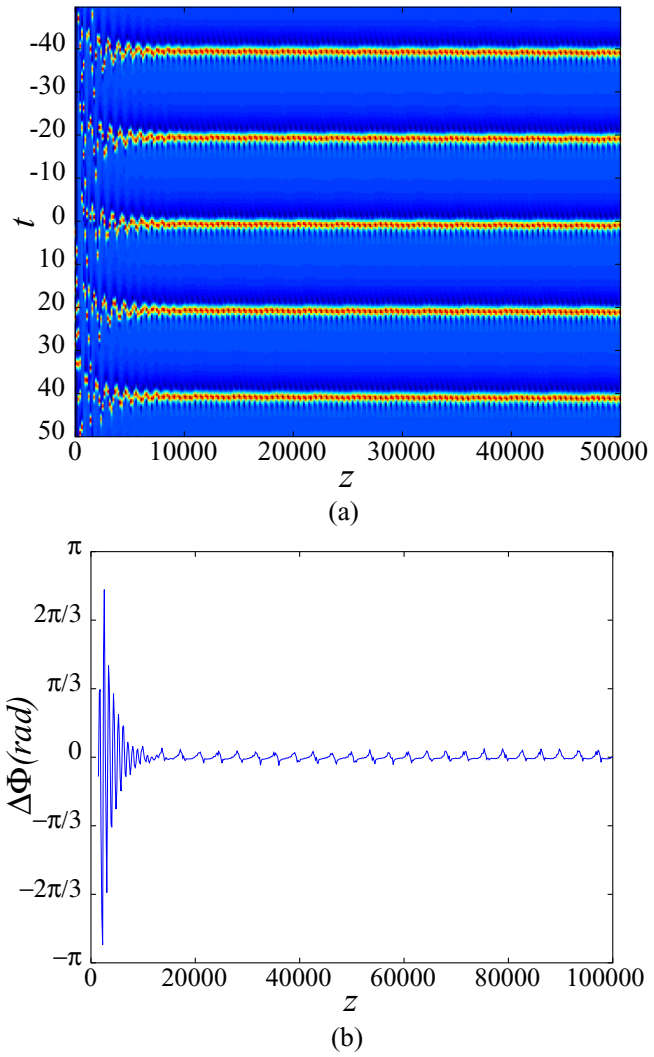

FIG. 7. (Color online) (a) Evolution of the temporal pattern toward harmonic mode locking, $\Delta\nu_0 = 0.1$, $A = 0.130$, $w = -0.027\,55$. (b) A typical example of the phase difference $\Delta\Phi$ between two consecutive pulses.

the whole computation box and become stable and equidistant. Such distribution of pulses occurs up to $A = 0.133$. Figure 7 shows such a distribution for $A = 0.130$. It is harmonic mode locking. The phase difference between consecutive solitons is shown in Fig. 7(b): After some transient state, the phase differences lock to zero. The train is phase locked. The present situation is thus simultaneously harmonic mode locking and a bounded state. The optical spectrum (Fig. 8) is strongly modulated, as expected for a coherent multiple pulse state. From $A = 0.134$ on, the number of solitons in the numerical box increases. It goes from 5 to 6 for $A = 0.134$. Then it further grows with the amplitude of the injected wave, while the distance between pulses decreases, up to 13 identical and equidistant pulses for $A = 0.270$. When the 14th soliton appears for $A = 0.280$, the harmonic mode locking ceases, a soliton gas beginning to form. As said above, it is not, properly speaking, the soliton gas observed in the fiber laser, since a substantial part of the power is given by the injected continuous wave.

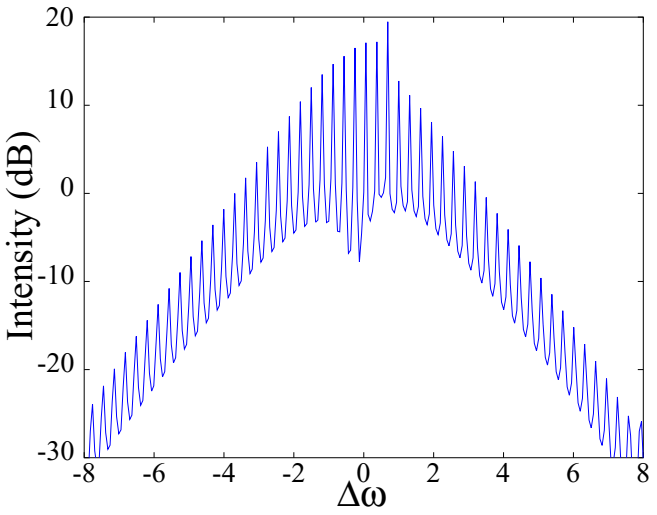

FIG. 8. (Color online) Optical spectrum of the harmonic mode locking, $\Delta\nu_0 = 0.1$ and $A = 0.130$.

We fix now the amplitude of the injected wave ($A = 0.130$) and vary the frequency shift $\Delta\nu_0$. The harmonic mode locking of the five pulses occurs between $\Delta\nu_0 = 0.0987$ and $\Delta\nu_0 = 0.1012$.

A strong periodic perturbation of the structure of the train is observed. This kind of jitter is related to the instants where a soliton crosses the boundary of the computation box. It will be discussed thereafter. It vanishes for the particular value of the frequency shift $\Delta\nu_0 = 0.0999$.

When the frequency shift of the injected component is relatively small ($0 \leq \Delta\nu_0 \leq 0.0987$) for an amplitude $A = 0.130$, the number of solitons in the box can vary. It can be less than the initial number of solitons (four pulses for $\Delta\nu_0 = 0$), more than it (seven or eight pulses for $\Delta\nu_0 = 0.09$), or the same as it (for $\Delta\nu_0 = 0.06$). Increasing the frequency shift $\Delta\nu_0$, the same features are obtained, but for higher amplitudes A. This is quite natural: We can expect that, closer to the resonance, less injected power is required to yield comparable effects. Note that the pulses are not always regularly spaced. For a frequency shift just above the domain where the five pulse harmonic mode-locking exists (more specifically, between $\Delta\nu_0 = 0.1013$ and $\Delta\nu_0 = 0.110$), we can get a system of six pulses in harmonic mode-locking regime.

For relatively large frequency shifts $\Delta\nu_0$, we find distributions similar to the behavior observed with varying the amplitude, but other kind of distributions too. Indeed, it may happen that the bound state of solitons breaks up, while the total number of solitons remains the same. Another issue is that the number of solitons may decrease in the cavity, down to four, three, or two. A few examples are shown in Fig. 9. The pulses are locked in position for $\Delta\nu_0 = 0.7$ and $\Delta\nu_0 = 1.0$ [Figs. 9(c) and 9(d)]. In the distributions presented in Fig. 9, the pulses are never phase locked.

VI. JITTER

In the harmonic mode-locking regime, strong oscillations of the pulse locations are observed. The pulses are in motion for an appreciable inverse speed, with respect to the frame in

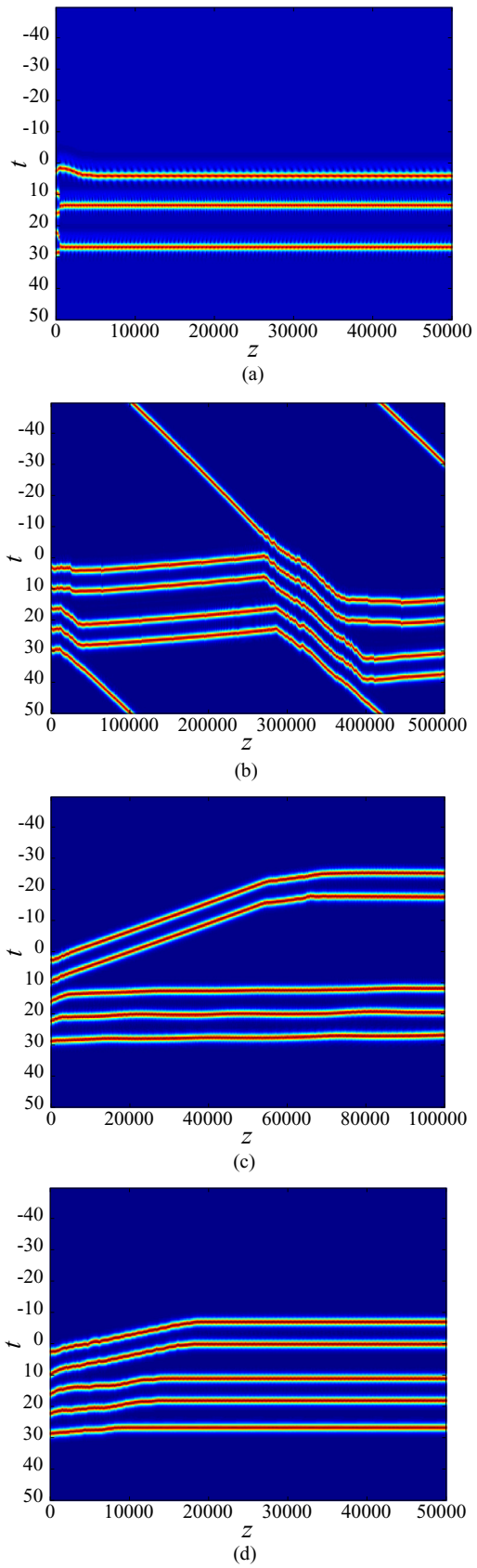

FIG. 9. (Color online) Examples of temporal distributions for different frequency shifts and a fixed amplitude ($A = 0.130$). (a) $\Delta\nu_0 = 0.2$ and $w = 0$; (b) $\Delta\nu_0 = 0.5$ and $w = -0.0024$; (c) $\Delta\nu_0 = 0.7$ and $w = -0.0005$; (d) $\Delta\nu_0 = 1.0$ and $w = 0$.

which Eq. (1) is written, which is, recall, the frame moving at the velocity of the linear monochromatic waves at the central frequency (corresponding to $\Delta\nu_0 = 0$). The inverse speed w corresponds to a shift in the group velocity due to nonlinear and nonconservative effects and mainly the gain dynamics. Recall that the above figures are presented in the frame which moves at the effective velocity of the stationary soliton pattern. However, in the initial frame, due to the velocity shift and periodicity, the pulses cross frequently the boundaries of the computation box.

The gain dynamics term is not symmetric as t is changed into $-t$, but tends to be monotonic, while the boundary conditions force it to be periodic. As a result, it varies faster in the vicinity of this boundary, which induces a strong perturbation in the soliton speed as it crosses it. This effect appears as a periodical perturbation of the pulse train in the frame moving at its own velocity.

The periodic boundary conditions might represent the fact that the real cavity makes a loop, and a physical meaning can be given to the effect we just mentioned. The pulses form a train in which the distance between them is fixed by the interactions. Each pulse uses some amount of gain. The gain must be recovered after one round trip, it is the gain-loss balance required for the laser to operate. This physical condition is taken into account in the model by the periodic boundary condition imposed to the gain dynamics term. Some amount of gain is recovered in the interval between two pulses, but the speed at which it is recovered mainly depends on the amplitude profile. After the train, there remains gain to be recovered in the remaining time. If the mismatch is important, it creates a strong disturbance in the gain profile, which, in turn, results in a disturbance in the amplitude profile. This causes some kind of jitter.

However, there is an appreciable discrepancy in the order of magnitude of the cavity length of a real fiber laser and that of the computation box. Further, the bounds of the real cavity are not fixed in the frame moving at the linear group velocity, but in the laboratory frame. Hence, although the periodic boundary conditions might in some cases be interpreted as representing qualitatively the finite length of the real cavity, no quantitative correspondence can be expected.

It seems that the pulse train, even in the harmonic mode-locking regime, has some eigenperiod τ, the characteristic value of the separation between pulses, independently of the box length T. It is characterized by the dynamics of gain consumption and recovery [20]. If the ratio T/τ is exactly an integer, the pulse train is periodic, and so is the gain, including the gain dynamics term. If T/τ is not an integer, the gain recovery at the end of the train must be either faster or slower than between two pulses. This yields a strong perturbation in the gain value about this point, which induces a local change in the pulse velocity (see Fig. 10; the inverse speed corrected in the figure was here $w = -0.013\,70$). This can be considered a dislocation of the soliton "crystal" and appears as a jitter.

For a particular value of parameters, the inverse velocity may vanish (for $T = 133.804$, same parameters as above; the inverse speed is $w = -0.000\,35$ only), then the oscillations vanish too.

It can be a physical effect, when one attempts to fill the entire cavity with a soliton crystal, such a dislocation can be expected somewhere in the pulse train. However, if the

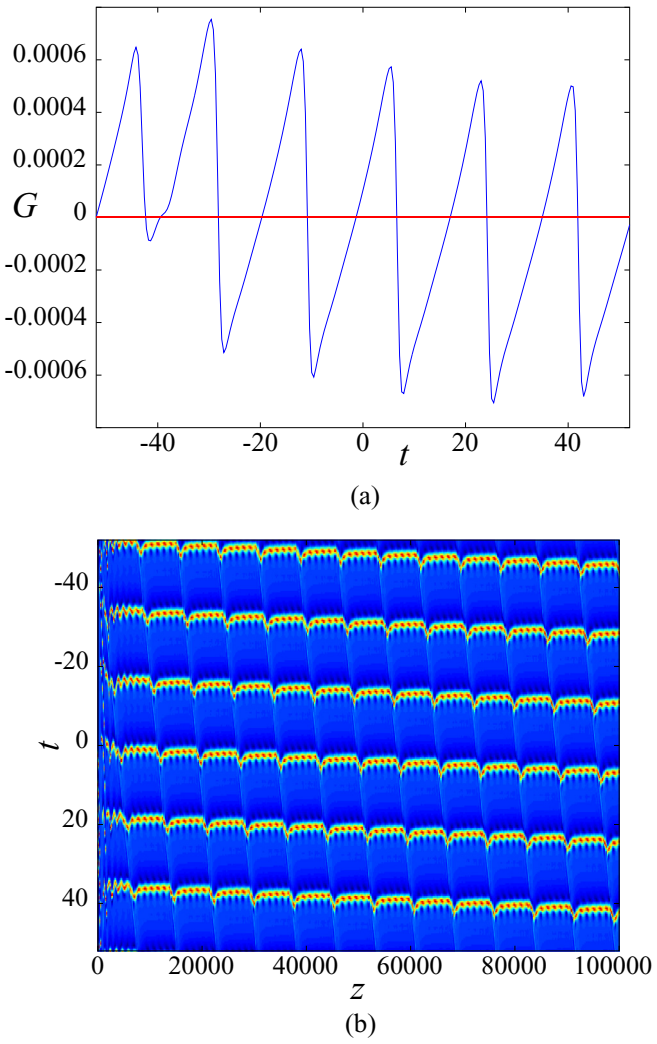

FIG. 10. (Color online) (a) An example of the dynamics gain profile in the harmonic mode-locking regime: The dynamic gain shift $G = -\Gamma \int^t (|E|^2 - \langle |E|^2 \rangle) dt'$ vs time t. (b) Oscillations of the soliton pattern due to the gain variations. Parameters: $T = 104$, $\Delta\nu_0 = 0.099$, $A = 0.13$, $w = -0.01370$.

numerical cavity is strongly increased, the effect becomes much smaller and almost not perceivable. Hence, it cannot occur in a fiber laser of several meters length as it appears in calculations.

We have observed the exact matching of T/τ; for $\Delta\nu_0 = 0.0999$ and $T = 100$, the inverse speed does not vanish ($w = -0.027\,55$), but there are no oscillations (even less than for $\Delta\nu_0 = 0.1$). For $\Delta\nu_0 = 0.1001$, and same parameters, the oscillations are already appreciable.

Another type of jitter, independent of the boundary, and consisting of oscillations of the train which do not originate in the box length, can also arise. For $T = 134.27$, e.g., and same parameters (see Fig. 11), the period of oscillations is about 1935, while the propagation distance for a pulse making one round trip in the box is about 9300. The two values are not commensurable. Here the origin of the oscillations differs from the mechanism described above and which was related to the box size: It is a true jitter. These oscillations can be considered

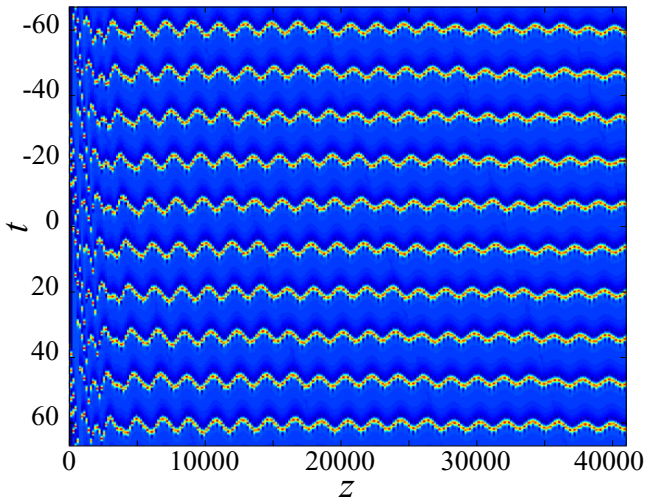

FIG. 11. (Color online) Jitter: oscillations of the soliton pattern which are not related with the box size. $T = 134$, $\Delta\nu_0 = 0.099$, $w = -0.014\,75$.

as a wave propagating along the pulse train in the transverse direction. However, in the frame which moves at the group velocity of the train, all pulses oscillate in phase: The velocity of the transverse wave coincides with the group velocity of the pulse train. The ratio of the amplitude of the oscillations to the pulse separation is here $\Delta\tau/\tau \simeq 14\%$. We thus identified two types of jitter, one of which is related to the matching between some proper period of the pulse train and the cavity length. Both types of oscillations may arise simultaneously.

VII. CONCLUSION

We investigated the effect of the gain dynamics on the collective behavior of solitons in the frame of a CGL-type model which represents dissipative soliton formation and propagation in a ring fiber laser. By itself, the gain dynamics induces a shift in the soliton velocity and can modify the properties of the interaction between pulses. An injected continuous wave also influences pulse velocity and interactions, and we investigate the effect of both together. We ran numerical solution of the model equation, starting from a bound state of a few solitons, which represents the crystal state, and changing the parameters of the continuous wave, and see that the outcomes are various. The initial bound state can be dislocated into a few bunches or into isolated pulses. Due to the periodicity, the splinters may interact; quasielastic collisions analogous to Newton's cradle have been seen. Irregularly evolving multisoliton states, of the liquid or gas type, can be produced. For rather specific values of the parameters, the pulse-pulse interaction becomes almost purely repulsive, and a harmonic mode-locking pattern can form. However, phase locking was conserved in the investigated examples.

The harmonic-mode-locking pattern presents almost always some jitter. It has been seen that it is often linked to the mismatch between natural train length and numerical cavity length. However, when these two quantities are perfectly matched, another type of jitter may appear.

[1] F. Amrani, A. Haboucha, M. Salhi, H. Leblond, A. Komarov, P. Grelu, and F. Sanchez, Passively mode-locked erbium-doped double-clad fiber laser operating at the 322nd harmonic, Opt. Lett. **34**, 2120 (2009).

[2] J. M. Dudley, G. Genty, and S. Coen, Supercontinuum generation in photonic crystal fiber, Rev. Mod. Phys. **78**, 1135 (2006).

[3] C. Lecaplain, Ph. Grelu, J. M. Soto-Crespo, and N. Akhmediev, Dissipative Rogue Waves Generated by Chaotic Pulse Bunching in a Mode-Locked Laser, Phys. Rev. Lett. **108**, 233901 (2012).

[4] A. Niang, F. Amrani, M. Salhi, H. Leblond, A. Komarov, and F. Sanchez, Harmonic mode-locking in a fiber laser through continuous external optical injection, Opt. Commun. **312**, 1 (2014).

[5] F. Amrani, A. Haboucha, M. Salhi, H. Leblond, A. Komarov, and F. Sanchez, Dissipative solitons compounds in a fiber laser. Analogy with the states of the matter, Appl. Phys. B **99**, 107 (2010).

[6] F. Amrani, M. Salhi, H. Leblond, and F. Sanchez, Characterization of solitons compounds in a passively mode-locked high power fiber laser, Opt. Commun. **283**, 5224 (2010).

[7] F. Amrani, M. Salhi, P. Grelu, H. Leblond, and F. Sanchez, Universal soliton pattern formations in passively mode-locked fiber lasers, Opt. Lett. **36**, 1545 (2011).

[8] S. Chouli and P. Grelu, Rains of solitons in a fiber laser, Opt. Express **17**, 11776 (2009).

[9] F. Amrani, A. Niang, M. Salhi, H. Leblond, and F. Sanchez, Passive harmonic mode locking of soliton crystals, Opt. Lett. **36**, 4239 (2011).

[10] G. Sobon, K. Krzempek, P. Kaczmarek, K. M. Abramski, and M. Nikodem, 10 GHz passive harmonic mode-locking in Er-Yb double-clad fiber laser, Opt. Commun. **284**, 4203 (2011).

[11] Z. X. Zhang, L. Zhan, X. X. Yang, S. Y. Luo, and Y. X. Xia, Passive harmonically mode-locked erbium-doped fiber laser with scalable repetition rate up to 1.2 GHz, Laser Phys. Lett. **4**, 592 (2007).

[12] S. Wabnitz, Optical turbulence in fiber lasers, Opt. Lett. **39**, 1362 (2014).

[13] H. Leblond, A. Niang, F. Amrani, M. Salhi, and F. Sanchez, Motion of solitons of the complex Ginzburg-Landau equation: The effect of an external frequency shifted source, Phys. Rev. A **88**, 033809 (2013).

[14] A. Komarov, H. Leblond, and F. Sanchez, Passive harmonic mode-locking in a fiber laser with nonlinear polarization rotation, Opt. Commun. **267**, 162 (2006).

[15] H. Leblond, M. Salhi, A. Hideur, T. Chartier, M. Brunel, and F. Sanchez, Experimental and theoretical study of the passively mode-locked Ytterbium-doped double-clad fiber laser, Phys. Rev. A **65**, 063811 (2002).

[16] M. Salhi, A. Haboucha, H. Leblond, and F. Sanchez, Theoretical study of figure-eight all fiber laser, Phys. Rev. A **77**, 033828 (2008).

[17] H. A. Haus, K. Tamura, L. E. Nelson, and E. P. Ippen, Stretched-pulse additive pulse mode-locking in fiber ring lasers: theory and experiment, IEEE J. Quantum Electron. **31**, 591 (1995).

[18] A. Komarov, H. Leblond, and F. Sanchez, Quintic complex Ginzburg-Landau model for ring fiber lasers, Phys. Rev. E **72**, 025604(R) (2005).

[19] E. Ding and J. N. Kutz, Operating regimes, split-step modeling, and the Haus master mode-locking model, J. Opt. Soc. Am. B **26**, 2290 (2009).

[20] A. Haboucha, H. Leblond, M. Salhi, A. Komarov, and F. Sanchez, Analysis of soliton pattern formation in passively mode-locked fiber lasers, Phys. Rev. A **78**, 043806 (2008).

[21] V. Besse, H. Leblond, D. Mihalache, and B. A. Malomed, Pattern formation by kicked solitons in the two-dimensional Ginzburg-Landau medium with a transverse grating, Phys. Rev. E **87**, 012916 (2013).

[22] R. Driben, B. A. Malomed, A. V. Yulin, and D. V. Skryabin, Newtons cradles in optics: From N-soliton fission to soliton chains, Phys. Rev. A **87**, 063808 (2013).